Photochemistry and Photobiology, 2009, 85: 387–390

Neuromelanins Isolated from Different Regions of the Human Brain Exhibit a Common Surface Photoionization Threshold

William D. Bush[1], Jacob Garguilo[1], Fabio A. Zucca[2], Chiara Bellei[2], Robert J. Nemanich[3], Glenn S. Edwards[4], Luigi Zecca[2] and John D. Simon*[1]

[1]Department of Chemistry, Duke University, Durham, NC
[2]Institute of Biomedical Technologies, Italian National Research Council, Segrate, Milan, Italy
[3]Department of Physics, Arizona State University, Tempe, AZ
[4]Department of Physics, Duke University, Durham, NC

Received 2 September 2008, accepted 17 September 2008, DOI: 10.1111/j.1751-1097.2008.00476.x

ABSTRACT

Neuromelanin isolated from the premotor cortex, cerebellum, putamen, globus pallidus and corpus callosum of the human brain is studied by scanning probe and photoelectron emission microscopies and the results are compared with previously published work on neuromelanin from the substantia nigra. Scanning electron microscopy reveals common structure for all neuromelanins. All exhibit spherical entities of diameters between 200 and 400 nm, composed of smaller spherical substructures, ~30 nm in diameter. These features are similar to that observed for many melanin systems including *Sepia* cuttlefish, bovine eye, and human eye and hair melanosomes. Photoelectron microscopy images were collected for all neuromelanins at specific wavelengths of ultraviolet light between 248 and 413 nm, using the spontaneous emission output from the Duke free electron laser. Analysis of the data establishes a common threshold photoionization potential for neuromelanins of 4.7 ± 0.2 eV, corresponding to an oxidation potential of −0.3 ± 0.2 V *vs* the normal hydrogen electrode (NHE). These results are consistent with previously reported potentials for neuromelanin from the substantia nigra of 4.5 ± 0.2 eV (−0.1 ± 0.2 V *vs* NHE). All neuromelanins exhibit a common low surface oxidation potential, reflecting their eumelanic component and their inability to trigger redox processes with neurotoxic effect.

INTRODUCTION

Neuromelanin is a naturally occurring pigment deposit found in the human central nervous system (1). Detectable levels of neuromelanin are observed in children approximately 3–5 years after birth, and the concentration of neuromelanin increases with age (2,3). There has been great emphasis on the study of neuromelanin isolated from the dopamine-producing neurons of the substantia nigra region in the human midbrain (4–6) because it is in this region that pigmented dopaminergic neurons are selectively degraded with the onset and progression of Parkinson's disease. As a result, pathological analysis reveals reduced concentration of neuromelanin in the substantia nigra of Parkinson's patients, relative to normal subjects (2,7). Although several hypotheses have been proposed, a direct link between the presence of neuromelanin and the pathophysiology of Parkinson's disease has been only partially clarified (8–10). Studies of neuromelanin reveal both neurotoxic and neuroprotective roles. Neuromelanin chelates redox-active metal ions thereby preventing their potential neurotoxic effect. Neuromelanin synthesis in the substantia nigra is a protective mechanism for neurons as it removes neurotoxic quinones, lending support to neuromelanin being a cellular defense mechanism against high oxidative stress (11–13). Neuromelanin could also be a source of toxic free radicals and redox-active compounds as pigmented neurons are degraded, which would, in contrast, serve to perpetuate oxidative stress and cytotoxicity in a cyclical fashion (12,14). This balance between mitigating and enhancing oxidative stress, and the factors that determine this balance are at the core of understanding the contribution(s) of neuromelanin to the neurodegenerative processes involved in the onset and progression of Parkinson's disease.

We recently reported the surface photoionization threshold for human neuromelanin from the substantia nigra to be 4.5 eV (15). This corresponds to an oxidation potential of −0.1 V *vs* the normal hydrogen electrode (NHE) (16). Herein, we extend this approach to determine the thresholds, and hence surface oxidation potentials for neuromelanin present in other regions of the human brain. Specifically, the neuromelanins isolated from the premotor cortex, cerebellum, putamen, corpus callosum and globus pallidus are examined.

With the exception of the corpus callosum these brain regions taken together are predominantly responsible for control over the coordinated movement of the human body and have different types of neurons. Corpus callosum has only glial cells and no neurons and is responsible for interhemispheric communications. The primary symptoms of Parkinson's disease are related to dopamine decrease in the putamen and caudatum and loss of synapsis formed by cortical and nigral projections in these regions (17). Additionally, the neural circuitry of motor control links the cerebellum with the motor cortex and, ultimately, with the basal ganglia. Therefore, each of the brain regions from

*Corresponding author email: jsimon@duke.edu (John D. Simon)

which neuromelanin is studied herein, with the exception of the corpus callosum as a control region, has been selected for its integral role in movement control, which is known to deteriorate in Parkinson's patients. The present study determines the relationship between the surface oxidation potential of neuromelanin from the substantia nigra and neuromelanin found in other regions of the human brain, especially those also involved in motor control but not selectively targeted in the pathology of Parkinson's disease.

MATERIALS AND METHODS

Sample preparation. Neuromelanins were isolated as reported previously (2). Samples were stored in a dessicator and protected from light. Samples for photoelectron emission microscopy (PEEM) analysis were prepared as follows. Sections of (100)-oriented silicon wafers (n-type, P-doped, low resistivity 0.005–0.01 Ω-cm; Virginia Semiconductor, Fredericksburg, VA) were cleaved into 9 × 9 mm squares after scribing with a diamond-tipped scribe and were cleaned by the standard (RCA) wet chemical procedure prior to deposition of neuromelanin on the surface. The hydrofluoric acid step was not included in our preparation as we desire a thin oxide layer for optimal sample deposition, therefore this procedure results in a surface terminated with a ~1 nm thick silicon oxide layer. All chemicals for the Si wafer RCA cleaning procedure (1 M HCl, 30% H_2O_2, 30% NH_4OH, 18 M H_2SO_4) were purchased from Fisher Chemical (Fairlawn, NJ) of the highest purity available. The wafers were dried over lens paper in a sterile petri dish while flowing argon gas over them. Neuromelanin samples were subsequently deposited onto the hydrophilic surface of the freshly RCA-cleaned Si wafer by micropipetting 0.5 μL of a neuromelanin suspension in doubly-distilled water (>18.2 MΩ) obtained from a Simplicity™ system (Millipore, Billerica, MA). Samples were dried in air at room temperature while being protected from light for less than 1 h prior to experimentation. This preparatory process was repeated immediately prior to each new experiment.

Scanning electron microscopy (SEM). Samples were prepared for SEM by using the same procedure as the one used for PEEM samples (as described above). Once prepared, the Si wafers containing a dried neuromelanin film were mounted on stainless steel pegs by double stick copper tape prior to being transferred to the SEM chamber. The mounted samples were coated with Au/Pd mist under argon plasma for 4 min at 10 mA using a Hummer V sputter coater (Anatech, Springfield, VA). A Philips FEI XL30 SEM-FEG (FEI Company, Portland, OR) equipped with a back-scattering secondary electron detector and a resolution of ~3 nm was used to examine the samples in ultrahigh resolution mode. The typical electron beam conditions were 3–5 kV, with a spot size of 3.0 mm, and a working distance of 4.0–6.0 mm. SEM images were captured and analyzed using analySIS™ XL DOCU software (Soft Imaging Systems, Lakewood, CO). All images were saved as .TIFF files.

Photoelectron emission microscopy. The Duke free electron laser and PEEM apparatus have been described in detail previously (18). We detected the photoelectron emission intensity of our neuromelanin samples within the spectral range of 248–413 nm (5.0–3.0 eV), using the spontaneous emission mode of the free electron laser with an energy full width at half maximum of ±0.1 eV. All PEEM images were acquired using a DVC 1312 M digital camera from DVC Company, Inc. (Austin, TX). The resolution of the digital camera is 1300 × 1030 pixels × 12 bits. The DVC View program was used to view/save images. After sample preparation (as described above), samples were always immediately transferred under ultrahigh vacuum into the PEEM chamber for the collection of data, with minimal exposure to ultraviolet radiation. We typically imaged large neuromelanin aggregates at fields of view in the PEEM of 150 μm, and smaller neuromelanin assemblies at fields of view of 5 or 1.5 μm. The focusing of the laser was optimized for each wavelength used, and the laser spot size on the sample was ~30 × 100 μm. The details of the methods of PEEM image analysis have been published elsewhere. The photoionization threshold, χ, is determined from a fit of the wavelength-dependent integrated brightness, $S(\lambda)$, of the image to the Fowler equation (19):

$$S(\lambda) = AT^2 f\left(\frac{h\nu - \chi}{k_B T}\right) \quad (1)$$

In the above expression, A is a proportionality constant, T is the temperature at which the experiments are conducted, k_B is the Boltzmann constant and

$$f(\mu) = e^{\mu} - \frac{e^{2\mu}}{2^2} + \frac{e^{3\mu}}{3^2} - \cdots, \quad \mu \le 0$$

$$= \frac{\pi^2}{6} + \frac{1}{2}\mu^2 - \left[e^{-\mu} - \frac{e^{-2\mu}}{2^2} + \frac{e^{-3\mu}}{3^2}\right], \quad \mu \ge 0.$$

RESULTS AND DISCUSSION

Scanning electron microscopy

Figure 1 shows SEM images of neuromelanins isolated from the premotor cortex, cerebellum, globus pallidus, putamen and corpus callosum. These samples reveal similar morphological characteristics, and are similar to our previously reported results on neuromelanin from the substantia nigra (15). Two types of structures are revealed by the imaging studies. For all the neuromelanins studied, spherical granules are observed, with diameters of 200–400 nm. Second, smaller spherical substructures, ~30 nm in diameter, are observed in all cases. The small particles could be found in aggregates of varying dimensions and also seen on the surfaces of the larger granules.

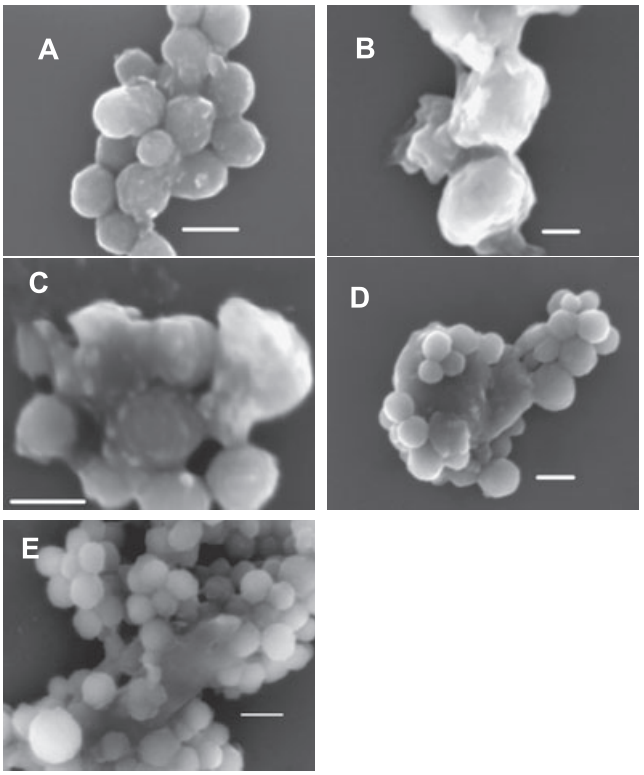

Figure 1. SEM images of neuromelanin pigments extracted from different regions of the human brain: (A) Premotor cortex; (B) cerebellum; (C) globus pallidus; (D) putamen; (E) corpus callosum. White scale bars in each image represent 200 nm.

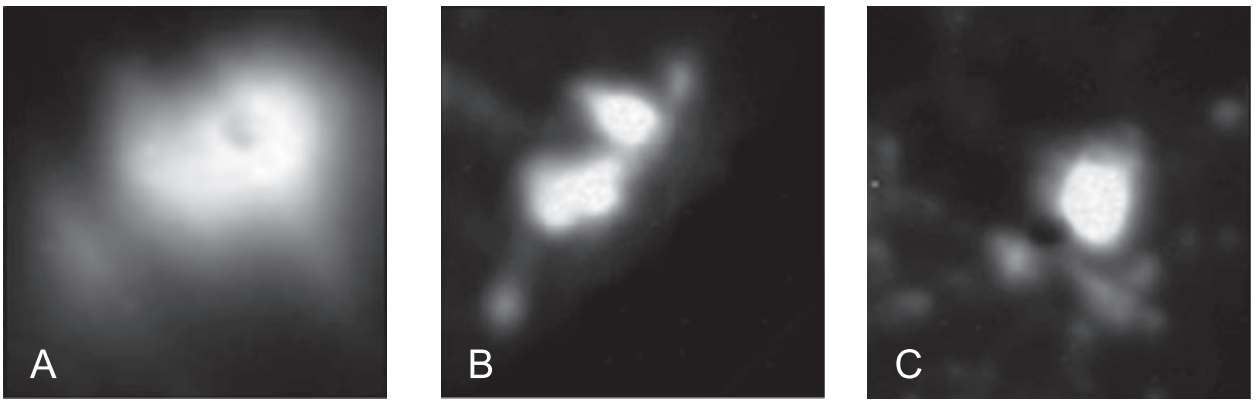

Figure 2. Examples of PEEM images of neuromelanin pigments used to determine photoionization thresholds. (A) Premotor cortex (500 nm × 500 nm); (B) cerebellum (1.25 μm × 1.25 μm); (C) putamen (1.25 μm × 1.25 μm). These images show that the thresholds are determined from an aggregate of neuromelanin granules, not from the analysis of individual granules.

Such small-scale substructure for melanin pigments has been previously reported for many natural melanins, including *Sepia* (20), human hair melanosomes (21), bovine ocular melanosomes (22) and human ocular melanosomes (23).

Threshold photoionization potentials

Wavelength-dependent PEEM has been successfully used to determine the threshold potentials of melanosomes from human hair (24,25), sepia melanosomes containing various concentrations of Fe(III) (26), and human ocular pigments—retinal pigment epithelium melanosomes and lipofuscin (23), and neuromelanin from the substantia nigra (15). Figure 2 shows PEEM images of neuromelanin from the premotor cortex, cerebellum and putamen. From the wavelength-dependent integrated intensity of images of these neuromelanins, their threshold potentials can be determined. Figure 3 shows such a plot. The data were analyzed as described in Materials and Methods section above, and the resulting potentials are presented in Table 1. All neuromelanins examined exhibit a threshold photoionization potential of ~4.7 ± 0.2 eV, corresponding to an electrochemical oxidation potential of −0.3 ± 0.2 V *vs* NHE. Previously we reported that neuromelanin isolated from the substantia nigra had an ionization threshold of 4.5 ± 0.2 eV (15), which is within the error of the values determined for the neuromelanins from these other regions of the brain. We therefore conclude that all neuromelanin in the human brain has the same surface oxidation potential.

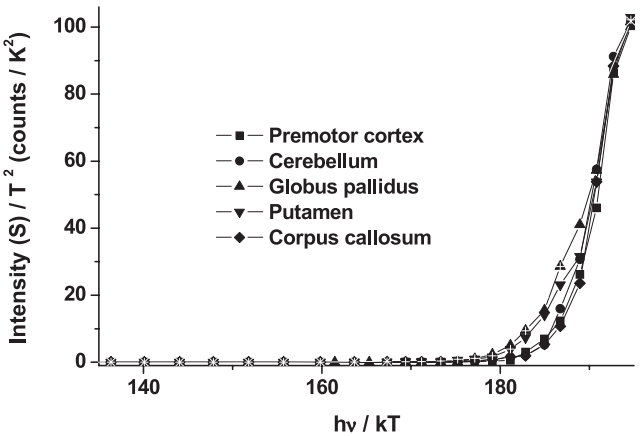

Figure 3. The spatially integrated intensity of the PEEM image of neuromelanin samples is plotted as a function of the excitation wavelength, and the data are fit according to Eq. (1). The determined photoionization threshold for the best fit curve to each experimental data set is presented in Table 1.

Table 1. Threshold photoionization potentials for neuromelanins isolated from different regions of the human brain.

Brain region	Threshold potential (eV)
Premotor cortex	4.7 ± 0.2
Cerebellum	4.7 ± 0.2
Globus pallidus	4.6 ± 0.2
Putamen	4.6 ± 0.2
Corpus callosum	4.6 ± 0.2
Substantia nigra (15)	4.5 ± 0.2

These observations are important in the broader context of the potential link of neuromelanins in Parkinson's disease, where the pigmented neurons of the substantia nigra are preferentially lost in the brains of Parkinson's patients. As stated above, the neuromelanins derived from the substantia nigra, basal ganglia, cerebellum and motor cortex brain regions come from regions containing a large number of neurons. These exhibit the same surface properties and also share common features with neuromelanin from the corpus callosum, a brain region containing only glial cells. This shows the presence of neuromelanin also in glial cells and not only in neurons, thus contrasting that claimed to date. From the standpoint of an understanding of the surface oxidation properties of neuromelanins, the intact, healthy neuromelanin contained within neurons cannot be responsible for the increased vulnerability of pigmented substantia nigra neurons. However, with degradation of neuromelanin granules, reactive cores can be exposed that can lead to substantial oxidative stress. It would be of great interest to elucidate the oxidation potential of neuromelanin isolated from affected and unaffected regions of the brain of Parkinson's patients.

Acknowledgements—J.D.S., G.S.E. and R.J.N. thank the AFOSR for support of this work through MFEL Grant FA9550-04-1-0086. F.A.Z., C.B. and L.Z. thank the Italian Fund for Basic Science (FIRB-MIUR) project RBNE03PX83_002 for support of this work, and the Lombardia Region Project Metadistretti-2005.

REFERENCES

1. Scherer, H. J. (1939) Melanin pigmentation of the substantia nigra in primates. *J. Comp. Neurol.* **71**, 91–98.
2. Zecca, L., R. Fariello, P. Riederer, D. Sulzer, A. Gotti and D. Tampellini (2002) The absolute concentration of nigral neuromelanin, assayed by a new sensitive method, increases throughout the life and is dramatically decreased in Parkinson's disease. *FEBS Lett.* **210**, 216–220.
3. Fenichel, G. M. and M. Bazelon (1968) Studies on neuromelanin II. Melanin in the brainstems of infants and children. *Neurology* **18**, 817–820.
4. Graham, D. G. (1979) On the origin and significance of neuromelanin. *Arch. Pathol. Lab. Med.* **103**, 359–362.
5. Zecca, L., A. Stroppolo, A. Gatti, D. Tampellini, M. Toscani, M. Gallorini, G. Giaveri, P. Arosio, P. Santambrogio, R. G. Fariello, E. Karatekin, M. H. Kleinman, N. Turro, O. Hornykiewicz and F. A. Zucca (2004) The role of iron and copper molecules in the neuronal vulnerability of locus coeruleus and substantia nigra during aging. *Proc. Natl Acad. Sci. USA* **101**, 9843–9848.
6. Zucca, F. A., G. Giaveri, M. Gallorini, A. Albertini, M. Toscani, G. Pezzoli, R. Lucius, H. Wilms, D. Sulzer, S. Ito, K. Wakamatsu and L. Zecca (2004) The neuromelanin of human substantia nigra: Physiological and pathogenic aspects. *Pigment Cell Res.* **17**, 610–617.
7. Gibb, W. R. (1992) Melanin, tyrosine hydroxylase, calbindin and substance P in the human midbrain and substantia nigra in relation to nigrostriatal projections and differential neuronal susceptibility in Parkinson's disease. *Brain Res.* **581**, 283–291.
8. Zecca, L., F. A. Zucca, P. Costi, D. Tampellini, A. Gatti, M. Gerlach, P. Riederer, R. G. Fariello, S. Ito, M. Gallorini and D. Sulzer (2003) The neuromelanin of human substantia nigra: Structure, synthesis and molecular behaviour. *J. Neural Transm. Suppl.* **65**, 145–155.
9. Wilms, H., P. Rosenstiel, J. Sievers, G. Deuschl, L. Zecca and R. Lucius (2003) Activation of microglia by human neuromelanin is NF-kappaB dependent and involves p38 mitogen-activated protein kinase: Implications for Parkinson's disease. *FASEB J.* **17**, 500–502.
10. Zecca, L., H. Wilms, S. Geick, J. H. Claasen, L. O. Brandenburg, C. Holzknecht, M. L. Panizza, F. A. Zucca, G. Deuschl, J. Sievers and R. Lucius (2008) Human neuromelanin induces neuroinflammation and neurodegeneration in the rat substantia nigra: Implications for Parkinson's disease. *Acta Neuropathol.* **116**, 47–55.
11. Zecca, L., T. Shima, A. Stroppolo, C. Goj, G. A. Battiston, R. Gerbasi, T. Sarna and H. M. Swartz (1996) Interaction of neuromelanin and iron in substantia nigra and other areas of human brain. *Neuroscience* **73**, 407–415.
12. Sulzer, D., J. Bogulavsky, K. E. Larsen, G. Behr, E. Karatekin, M. H. Kleinman, N. Turro, D. Krantz, R. H. Edwards, L. A. Greene and L. Zecca (2000) Neuromelanin biosynthesis is driven by excess cytosolic catecholamines not accumulated by synaptic vesicles. *Proc. Natl Acad. Sci. USA* **97**, 11869–11874.
13. Liang, C. L., O. Nelson, U. Yazdani, P. Pasbakhsh and D. C. German (2004) Inverse relationship between the contents of neuromelanin pigment and the vesicular monoamine transporter-2: Human midbrain dopamine neurons. *J. Comp. Neurol.* **473**, 97–106.
14. Zecca, L., F. A. Zucca, H. Wilms and D. Sulzer (2003) Neuromelanin of the substantia nigra: A neuronal black hole with protective and toxic characteristics. *Trends Neurosci.* **26**, 578–580.
15. Bush, W. D., J. Garguilo, F. A. Zucca, A. Albertini, L. Zecca, G. S. Edwards, R. J. Nemanich and J. D. Simon (2006) The surface oxidation potential of human neuromelanin reveals a spherical architecture with a pheomelanin core and a eumelanin surface. *Proc. Natl Acad. Sci. USA* **103**, 14785–14789.
16. Graetzel, M. (2001) Photoelectrochemical cells. *Nature* **414**, 338–344.
17. Fahn, S. and S. Przedborski (2005) Parkinsonism. In *Merritt's Neurology* (Edited by L. P. Rowland), pp. 828–846. Lippincott Williams & Wilkins, New York.
18. Ade, H., W. Yang, S. L. English, J. Hartman, R. F. Davis, R. J. Nemanich, V. N. Litvinenko, I. V. Pinayev, Y. Wu and J. M. J. Madey (1998) A free electron laser–photoemission electron microscope system (FEL–PEEM). *Surf. Rev. Lett.* **5**, 1257–1268.
19. Fowler, R. H. (1931) The analysis of photoelectric sensitivity curves for clean metals at various temperatures. *Phys. Rev.* **38**, 45–56.
20. Clancy, C. M. R. and J. D. Simon (2001) Ultrastructural organization of eumelanin from *Sepia officinalis* measured by atomic force microscopy. *Biochemistry* **40**, 13353–13360.
21. Liu, Y. and J. D. Simon (2003) The effect of preparation procedures on the morphology of melanin from the ink sac of *Sepia officinalis*. *Pigment Cell Res.* **16**, 1–13.
22. Liu, Y., L. Hong, K. Wakamatsu, S. Ito, B. B. Adhyaru, C. Y. Cheng, C. R. Bowers and J. D. Simon (2005) Comparisons of the structural and chemical properties of melanosomes isolated from retinal pigment epithelium, iris and choroid of newborn and mature bovine eyes. *Photochem. Photobiol.* **81**, 510–516.
23. Hong, L., J. Garguilo, L. Anzaldi, G. S. Edwards, R. J. Nemanich and J. D. Simon (2006) Age-dependent photoionization thresholds of melanosomes and lipofuscin isolated from human retinal pigment epithelium cells. *Photochem. Photobiol.* **82**, 1475–1481.
24. Samokhvalov, A., J. Garguilo, W. C. Yang, G. S. Edwards, R. J. Nemanich and J. D. Simon (2004) Photoionization thresholds of eumelanosomes determined by free electron laser–photoelectron emission microscopy. *J. Phys. Chem. B* **108**, 16334–16338.
25. Samokhvalov, A., L. Hong, Y. Liu, J. Garguilo, R. J. Nemanich, G. S. Edwards and J. D. Simon (2005) Oxidation potentials of human eumelanosomes and pheomelanosomes. *Photochem. Photobiol.* **81**, 145–148.
26. Garguilo, J., L. Hong, G. S. Edwards, R. J. Nemanich and J. D. Simon (2007) The surface oxidation potential of melanosomes measured by free electron laser–photoelectron emission microscopy. *Photochem. Photobiol.* **83**, 692–697.